

GaPSb non-random distribution within its site tetrahedron configurations: bond distances and coordination numbers

B.V.Robouch ^{a,*}, Hao-Hsiung Lin ^b, Jay Chou ^{b,*}, R.G. Valeev ^c, A.L. Trigub ^{c,d}, J. Omar ^e,
A. Kisiel ^f and A. Marcelli ^{a,g}

^a INFN - Laboratori Nazionali Frascati, via E. Fermi 40, CP 13, 00044 Frascati (RM), Italy

^b Department of Electrical Engineering and Graduate Institute of Electronics Engineering, National Taiwan University, No. 1, Sec. 4, Roosevelt Road, Taipei, 10617, Taiwan, hmlin@ntu.edu.tw

^c Physical-Technical Institute of Ural Branch of RAS, Kirova str. 132, Izhevsk 426000, Russia

^d National Research Centre 'Kurchatov Institute', 1 Akademika Kurchatova pl., 123182 Moscow, Russia

^e European Commission, Joint Research Centre, JRC-Geel, Retieseweg, 111 Geel, Belgium

^f Instytut Fizyki, Uniwersytet Jagielloński, Reymonta 4, 30-059 Cracow, Poland

^g RICMASS - Rome International Center for Materials Science Superstripes, Via Sabelli 119A, 00185 Roma, Italy

* Corresponding author - Email: robouch@lnf.infn.it; Tel.: +39.06.9403. 2218.

jaye5e5e5@gmail.com

Keywords: ternary alloys; site occupation preference; GaPSb 9 March 20189
March 20189 February 2018

Submit to XAFS2018 at Cracow?
by ALL

Abstract

1. Introduction

by ALL

GaPSb a ternary **B3** (sphalerite tetrahedron structured) alloy is under intense investigation [[1-9]] for its crystal particularities; relative property information is available [[10, 11]]. The two binary compounds GaP and GaSb from which it derives are characterized by highly mismatched in size bond-distances (R_1) $R_{1.GaP} = 2.360$ $R_{1.GaSb} = 2.641$ [Å]. In forming its tetrahedron configurations, this bond-mismatch introduces when packing into the alloy lattice, strong internal stretching and bending strains. This makes growing samples rather difficult. Although the strong bond distortion leads to difficulty in epitaxial growth, the distortion, especially the bending, strongly influences the electronic band structure.

The manuscript presents and discusses observed GaPSb spectra measured at the National Synchrotron Radiation Research Center (NSRRC) in Taiwan. Four samples were grown-in a local epi-house by Metal Organic Vapor Phase Epitaxy (**MOVPE**) with relative contents x_P , x_{Sb} (Table-1).

Table 1. Relative contents x_P , x_{Sb} of the four EXAFS investigated samples

Sample	A	B	C	D
x_P	0.64	0.71	0.94	0.71
x_{Sb}	0.36	0.29	0.06	0.29

Using the multivariate **PLS** (Partial Least Square Regression method) analysis [12] we identify the spectra that are statistically reliable and suitable for the *Iffffit* analysis [13]. From the *Iffffit*-obtained results, **SOP** (Site Occupation Preference) coefficients for tetrahedron configurations W_k ($0 \leq W_k \leq 4/k$) with $C_k = \min[W_k, 1, (4-k*W_k)/(4-k)] \leq 1$ (attenuation coefficient of $p^{[4]}_k$ - corresponding Bernoulli Eigenfunction), are determined using the Strained Tetrahedron Model [14-19].

The notion of preferences spontaneously derives from EXAFS, neutron scattering or FIR experiments of crystals. The present study represents the natural extension of a previous investigation on the **IPs** (Internal Preferences) [19] performed combining experimental observations of over twenty ternary systems and four pseudo quaternary alloys available in the literature [19]. For the **GaPSb** system we determine the ion distribution within its strained tetrahedra, with account of the non-random distribution

induced by SOPs. The non-negative probability of the SOP W_k factors account for the alloy's preferences relative to the distribution of the respective component elements over each other [19]. The $\text{GaP}_x\text{Sb}_{1-x}$, tetrahedron structured, canonically consists of five types of different elemental tetrahedra: ${}^{kP,jSb}T_k$ for $k=0,\dots,4$ (where k and $j=4-k$ are the number of anions P and Sb around the central cation Ga, respectively), two binary and three ternary configurations [18]. Remember that sphalerite binary configurations are perfectly symmetric, while ternary configurations are strained.

Within the framework of the *Strained Tetrahedron Model*, SOPs obtained quantify the attenuation of the *multinary* configurations accounting for the departure from the random Bernoulli values. The attenuation of the configurations listed above is characterized by the *attenuation index* $\sum_{k=1,N-1} C_k/(N-1)$, (where N is the number of Nearest Neighbor (NN) sites around the central ion), and for a tetrahedron configuration $N=4$. Depending on the intensity of SOPs, for a ternary system this index ranges from $\sum C_k/3 = 1$ (no attenuation) as in the case of the ternary alloy ZnCdTe [15] to $\sum C_k/3 = 0.05$ in the ZnSSe system, a special system in which an almost extreme attenuation of multinary configurations is observed [20].

1. Experimental section by Lin & Jay OK

Four GaPSb alloy samples were grown by MOVPE on 600 μm GaAs substrates. A 20 nm thick GaAs capping layer was grown following the alloy layer. The x_{Sb} values of all the $\text{GaP}_{1-x}\text{Sb}_x$ layers were determined by non-destructive high-resolution XRD measurements; in calculating, we assumed that the layers are coherent to the GaAs substrate and used Vegard's law to determine the values of x_{Sb} [21].

Four GaPSb samples were investigated in this work. The epilayers of the samples were grown on semi-insulating (001) GaAs substrates by MOVPE. The metal-organic sources were trimethylgallium and trimethylantimony, while the hydride sources were phosphine and arsine. Samples A, B, and C consist of double epilayer structures each, while sample D has two extra GaAs layers (Table 2).

Table 2. Structure of the four $\text{GaP}_{1-x}\text{Sb}_x$ sample layers.

Sample	Structure	Substrate	Si-doped GaAs $4 \times 10^{18} \text{cm}^{-3}$	Undoped GaAs	Alloy layer	Capping layer
	Material	S.I. GaAs			GaPSb	GaAs
	x_{Sb}	Thickness (μm)	Thickness (nm)	Thickness (nm)	Thickness (nm)	Thickness (nm)
A	0.06	600	0	0	350	20
B	0.29	600	0	0	700	20
C	0.36	600	0	0	700	20
D	0.29	600	500	300	210	300 (*)

(*) The capping layer of sample D was Si-doped with a density of $4 \times 10^{18} \text{cm}^{-3}$.

All samples were EXAFS (extended X-ray absorption fine structure) investigated at NSRRC. The P and Sb K-edge EXAFS spectra were measured at the experimental conditions reassumed in tabular form

Energy Range	2 ~ 8 keV (P K-edge: 2146 eV)	6 ~ 33 keV (Sb K-edge: 30491 eV)
Energy Resolution	$1.5 \sim 2.1 \times 10^{-4}$	2.3×10^{-4}
Photon Flux (photons/sec)	3×10^{11} (0.38 mW)	3×10^{10} (at 20 keV)
Spot Size (FWHM)	0.5 mm (H) x 0.4 mm (V)	0.9 mm (H) x 0.2 mm (V)
Detectors	Gas Ionization Chambers, Lytle Detector	

The observed signals are shown (Figures 1 and 2).

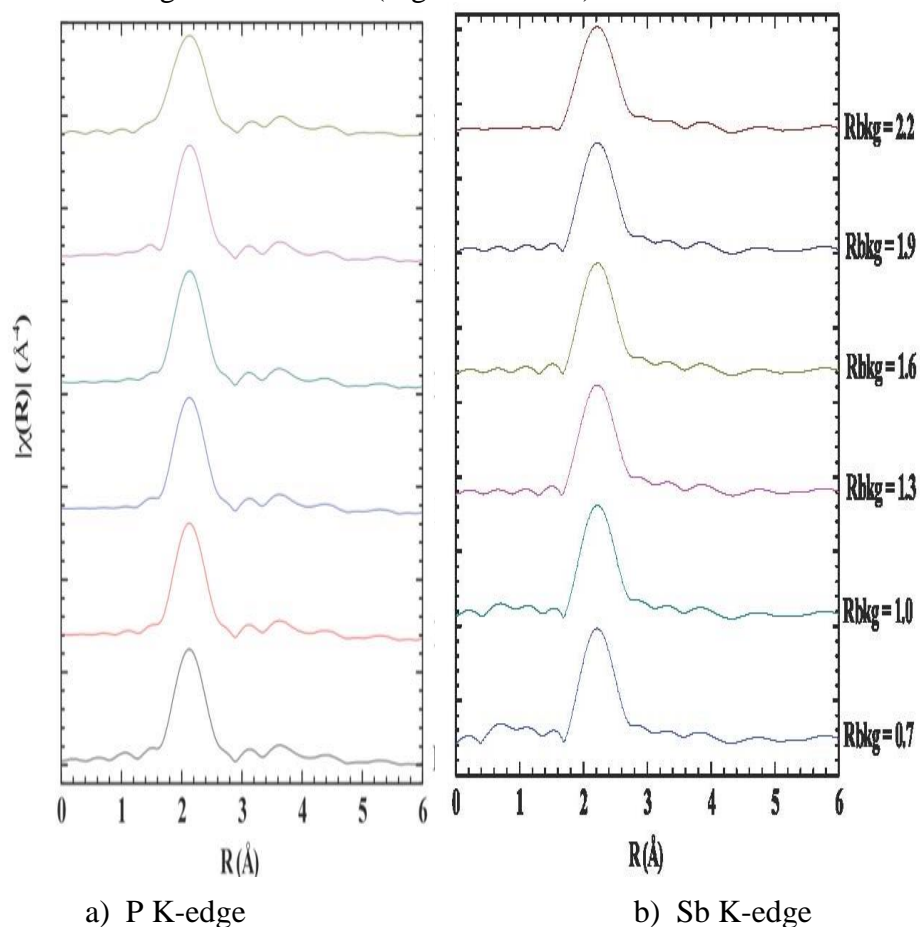


Fig.1 Sample B EXAFS spectra: $|\chi(R)|$ vs. Reduced distance (R) for various R_{bkg} (background removal) values at the a)-P and b)-Sb K-edges for $R_{bkg} = 0.7$ (0.3) 2.2

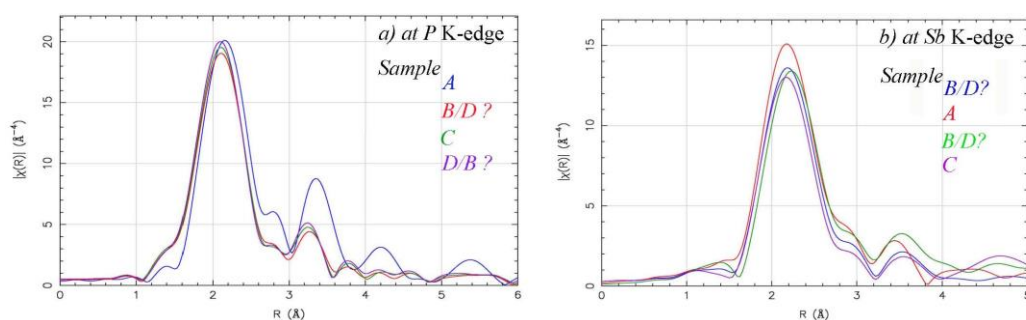


Fig. 2. EXAFS spectra: $|\chi(R)|$ vs. Reduced distance (R) for the four samples at K-edges of a) P and b) Sb

x_{sb}	Sample	
0.06	A	CA10119AK20555
0.29	B	CA10122AK80555
0.36	C	CA10122AK50555
0.29	D	CA10124AK10555

2. Multivariate analysis of the observed FT-spectra

by Jone

The statistical analysis [12]^{Kessler 2006} of the reported FT-spectra observes that ... at the ?? K-edge data are reliable and....

, [22]^{Brereton 2000 PCA}, [23]^{Gemperline 2006}

Fig. 2. Partial Least Square Regression (PLS) analysis of the P- Sb- K-edge spectra;

$$a) y = 0.87x_P + 0.06, R^2 = 0.97; b) y = 0.80x_{Sb} + 0.04, R^2 = 0.81.$$

3. Iffffit analysis of EXAFS spectra

by Valeev & Trigub

From the reliable spectra at the **P- Sb- K-edge** the Iffffit program recovers the N_1 - and R_1 -values assuming two independent N_1 parameters, $N_{1,P}$ $N_{1,Sb}$ with $N_{1,P} + N_{1,Sb} = 4$ (Table 2). While fitting, the standard quadratic deviations σ^2 of P and Sb atoms were recorded. Samples having been observed at room temperature, code FEFF-8 is calculated for 300 K Debye temperature.

Table 2. Coordination numbers ($N_1 \pm 0.1$) and bond distances ($R_1 \pm 0.01 \text{ \AA}$) as obtained from the **P and **Sb** K-edges.**

Binary	x_P	x_{Sb}	$N_{1,GaP}$	$N_{1,GaSb}$	$R_{1,GaP} (\text{\AA})$	$R_{1,GaSb} (\text{\AA})$
	1	0	4	0	2.360	=
	0	1	0	4	=	2.641
Ternary						
Sample						
A	0.64	0.36				
B	0.71	0.29				
C	0.94	0.06				
D	0.71	0.29				

4. Application of the Strained Tetrahedron Model

by BVR

The Strained Tetrahedron Model [17] was applied to analyze the available data of the GaP_xSb_{1-x} system. The SOP coefficients W_k and the attenuation factors C_k ($= \min[W_k, 1, (4-kW_k)/(4-k)] \leq 1$) of each random Bernoulli Eigen-function of the three canonical different possible ternary distorted tetrahedron configurations ${}^{kP/Sb}T_k$ are determined (Table 3). The procedure uses the equations previously developed and discussed [19]. Starting from the experimental values, Excel Solver was used to best fit the ternary parameters to determine the SOP W_k coefficients.

Table 3. W_k and C_k values of the three tetrahedron-configurations

Samples				
Type	k_P	j_{Sb}	W_k	C_k
Binary				
${}^4P T_4$	4	0	=	=
${}^4Sb T_0$	0	4	=	=
Ternary				
${}^1P^3Sb T_1$	1	3		
${}^2P^2Sb T_2$	2	2		
${}^3P^1Sb T_3$	3	1		
$\Sigma(C_k)/3 =$				

Fig. 3. Plot of the N_I and R_I values from the P- Sb- K-edge (from Table 2)

Results show that in our GaPSb samples as the P content increases, ...

The concept of Internal Preferences allows identifying preferences in the frame of distorted tetrahedra. ...

The integral of any Bernoulli Eigen-function N_p over the entire relative content $x = [0,1]$ range is $1/(N+1)$ [19].

The results of the analysis ...

$$\Delta P_{4P} = \sum_{k=0}^3 \left[\max(0, 1-W_k) + \max[0, k*(W_k-1)/(4-k)] \right]$$

Table 4. $\Delta P_{4P}/3$ and $\Delta P_{4Sb}/3$ integral values showing the binary fractions respect to the original Bernoulli values.

Binary	${}^4P T_i$	${}^4Sb T_i$
$\Sigma \Delta P/3$		

5. Conclusions

by ALL

From the Strained Tetrahedron Model we infer that the results obtained, although limited are extremely stimulating to understand this extremely complex ternary system containing gallium. Actually it would be useful to compare experimental EXAFS spectra with the spectra of the pure binary GaP compound. A deeper investigation of the XANES spectra of pure GaP could be useful to better evaluate the Sb chemical state in GaPSb alloys, the small local structural distortions vs. Sb in the second coordination shell, and using DFT ([Discrete Fourier transform](#)) calculations, charge effects due to Sb doping.

The bond lengths of the NN (nearest neighbors) tend to be almost the same at different Rbkg parameters

For P K-edge absorption, the bonding structure around the Ga tends to be 3P1Sb, and the fitting result is consistent with the VFF (valence force field) model.

For Sb K-edge absorption, the bonding structure around the Ga also tends to be 3P1Sb, but the fitting results of the NNN (next nearest neighbors) are not yet explainable.

Dear colleagues,

In attachment I summarized best experimental spectra, XANES and FT transformations of EXAFS spectra.

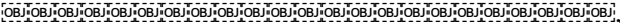
- It could be useful to compare EXAFS and XANES spectra of pure GaP and GaP_xSb_{1-x} . I have found old paper concerning XANES spectra of pure GaP. XANES spectra of pure GaP is almost the same like in our experimental data. [24]
There is an energy shift in edge position for samples with $x=0.29, 0.36$. In our case there is no changes in shape of XANES spectra, so energy shift could be assigned to increasing atomic charge of in atoms. For more precise estimations of charge effects of Sb doping, if it's necessary, DFT (Discrete Fourier transform) calculations could be done.
- Some changes in P XANES spectra are observed at 2150-2160 eV, there is some smoothing of the spectrum for almost pure $GaP_{0.06Sb_{0.94}}$. It could be explained like distortion of the local atomic symmetry for P atoms.
- All XANES spectra measured at Sb K-edge looks the same. This means that Sb atoms has identical charge state in all samples. It's useful to compare these XANES spectra with standards to validate Sb chemical state.
- In EXAFS spectra at P K-edge there is a shift of main peak at 2.2Å due to different size of P and Sb atoms. Decreasing of the peak at 3.4 Å could be attributed to appearance of Sb atoms in second coordination sphere for P. It would be greater to compare out experimental EXAFS spectra with EXAFS for pure GaP.
- In EXAFS spectra at Sb K-edge there is no significant changes, but they are also could be used to extract some information.
- There is two sets named $x_{Sb}=0.29$ in experimental file EFXAS data list-1.xlsx, they are the same?
- Is it available spectra for pure GaP?
For P K-edge absorption, the bonding structure around the Ga tends to be 3P+1Sb, because of the Coulomb interaction between Sb impurities.
If it's necessary, some calculations of XANES spectra could be done to demonstrate changes of the spectral shape with increasing amount of Sb atoms in second coordination shell for P atoms.
Hope, till the end of the next week some results of the EXAFS analysis will be ready.
Best regards, Alexander.

Acknowledgements

Authors acknowledge P. Robouch for his valuable comments and suggestions, and A. Grilli for his help in the setup of the figures of this manuscript.

References

- [1] M.J. Jou , T. Cherng, H.R. Jen, G.B. Stringfellow, Organometallic vapor phase epitaxial growth semiconductor alloy: $GaP_{1-x}Sb_x$, IEEE Xplore, (1988).
- [2] G.B. Stringfellow, Ordered structures and metastable alloys grown by OMVPE, Journal of Crystal Growth, 98 (1989) 108-117.
- [3] S. Loualiche, A. Le Corre, S. Salaun, J. Caulet, B. Lambert, M. Gauneau, D. Lecrosnier, B. Deveaud, GaPSb: A new ternary material for Schottky diode fabrication on InP, Appl. Phys. Lett., 59 (1991) 423-424.
- [4] I. Vurgaftman, J.R. Meyer, L.R. Ram-Mohan, Band parameters for III-V compound semiconductors and their alloys, JOURNAL OF APPLIED PHYSICS, 89 (2001) 5815-5875.
- [5] C. Grasse, R. Meyer, U. Breuer, G. Bo'hm, A. Markus-Christian, Growth of various antimony-containing alloys by MOVPE, Journal of Crystal Growth, 310 (2008) 4835-4838.

- [6] G.B. Stringfellow, Ordering in III/V Alloys, MRS Online Proceedings Library (OPL), 163 (Symposium G – Impurities, Defects and Diffusion in Semiconductors: Bulk and Layered Structures) (2011) 893.
- [7] Growth and structural characterization of GaP/Ga(P_{1-x}Sb_x) nanowires, in, Lunds Tekniska Hogskola, Lunds Universitet, 2013, pp. 50.
- [8] D. Chen, N.M. Ravindra, Structural, thermodynamic and electronic properties of GaP_xSb_{1-x} and InP_xSb_{1-x} alloys, Emerging Materials Research - Themed Issue Research Paper 2 (2013) 109-113.
- [9] H.B. Russell, A.N. Andriotis, M. Menon, J.B. Jasinski, A. Martinez-Garcia, M.K. Sunkara, Direct Band Gap Gallium Antimony Phosphide (GaSb_xP_{1-x}) Alloys, Scientific Reports 6(2016) 20822.
- [10] D.K. Ferry, R.O. Grondin, Physics of Submicron Devices, Springer Science & Business Media, 2012.
- [11] A. Editor: Mascarenhas, Spontaneous Ordering in Semiconductor Alloys, Springer, 2017.
- [12] W. Kessler, Multivariate Datenanalyse: für die Pharma-, Bio- und Prozessanalytik, 2006.
- [13] Ed. Matthew Newville, Iffeffit - IFEFFIT Version 1.2.5, in: Consortium for Advanced Radiation Sources, University of Chicago, Chicago, IL, 2004.
- [14] B.V. Robouch, A. Marcelli, M. Cestelli Guidi, A. Kisiel, E.M. Sheregii, J. Polit, J. Cebulski, M. Piccinini, A. Mycielski, V.I. Ivanov-Omskii, E. Sciesinska, J. Sciesinski, E. Burattini, Statistical model analysis of local structure of quaternary sphalerite crystals, Fizika Nizkikh Temperatur (Φ H T) 33, 291-303 (2007) - Low Temperature Physics, 33 (2007) 214-225.
- [15] B.V. Robouch, A. Kisiel, J. Konior, Statistical model for site occupation preferences and shapes of elemental tetrahedra in the zinc-blende type semiconductors GaInAs, GaAsP, ZnCdTe, Journal of Alloys and Compounds, 339 (2002) 1-17.
- [16] B.V. Robouch, A. Kisiel, J. Konior, Statistical model for atomic distances and site occupation in zinc-blende diluted magnetic semiconductors (DMSs), Journal of Alloys and Compounds, 340 (2002) 13-26.
- [17] B.V. Robouch, E.M. Sheregii, A. Kisiel, Statistical strained tetrahedron model of local ternary zinc blend crystal structures, Low Temp.Phys.30, 921-929 (2004), 30 (2004) 921-929.
- [18] B.V. Robouch, A. Marcelli, P. Robouch, A. Kisiel, Occupation preference values in doped CmIm' multinaries from EXAFS and FTIR correlative analysis, Fizika Nizkikh Temperatur (Φ H T) 37 (3) 308-312 (2011) - Low Temperature Physics, 37 (2011) 241-244.
- [19] A. Kisiel, B.V. Robouch, A. Marcelli, The status of art of the analysis of complex multinary semiconductor alloys, Opto–Electronics Review, In print (2017) pp.15.
- [20] R.G. Valeev, E.A. Romanov, V.I. Vorobiev, V.V. Mukhgalin, V.V. Kriventsov, A.I. Chukavin, B.V. Robouch, Structure and properties of ZnS_xSe_{1-x} thin films deposited by thermal evaporation of ZnS and ZnSe powder mixtures, Materials Research Express , 2 (2015) 9.
- [21] T. Fukui, Atomic structure model for Ga:1 - x h1x As saUd solution, Journal Appl. Physics, 57 (1985) 5188-5191.
- [22] R.G. Brereton, Introduction to multivariate calibration in analytical chemistry, The Royal Society of Chemistry - Analyst, 125 (2000) 2125-2154.
- [23] P. Gemperline, Practical guide to chemometrics, CRC Press - Taylor & Francis Group, Boca Raton, FL 33487-2742 USA, 2006.
- [24] H. Oizum, J. Junichi, H. Oyanagi, T. Fujikawa, T. Ohta, S. Usami, K-Edge XANES of GaP, InP and GaSb, Jpn. J. Appl. Phys. , 24 (1985) 1475-1478.